# ChemComm

Accepted Manuscript


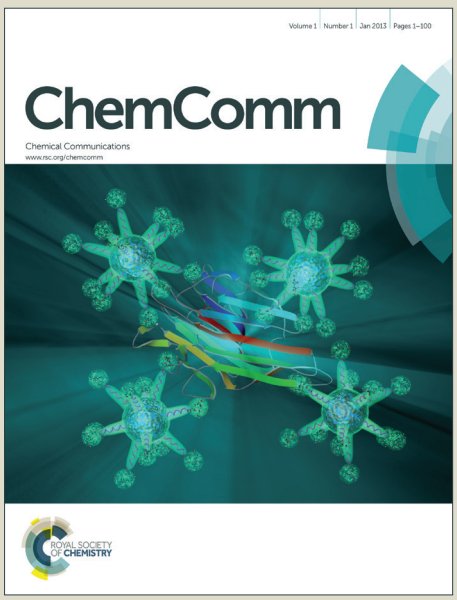





ROYAL SOCIETY OF CHEMISTRY

www.rsc.org/chemcomm

ChemComm

RSCPublishing

COMMUNICATION

# Surfactant-free Pd nanoparticles immobilized to metal-organic framework with size- and location-dependent catalytic selectivity

Cite this: DOI: 10.1039/x0xx00000x

Received ooth January 2014,
Accepted ooth January 2014

DOI: 10.1039/x0xx00000x

www.rsc.org/

Arshad Aijaz,[a] Qi-Long Zhu,[a] Nobuko Tsumori,[b] Tomoki Akita[a] and Qiang Xu[a]*

**Surfactant-free Pd nanoparticles, immobilized to metal-organic framework (MIL-101), have been used for the first time as a highly active and durable catalyst in water for biomass refining (hydrodeoxygenation of vanillin, a typical compound of lignin) with metal nanoparticle size- and location-dependent catalytic activity and selectivity.**

In recent years, catalysis using metal nanoparticles (MNPs) has attracted great interest in search of selective and enhanced catalytic performances.[1,2] Immobilizing MNPs to porous materials could afford heterogeneous catalysts having surfactant-free active sites with the advantages of controlling particle nucleation and growth to a nanosize region in the confined pores and reducing particle aggregation.[3] MOFs have particularly demonstrated their potentials for immobilizing fine MNPs within their pores for heterogeneous catalysis.[4,5] MOFs are crystalline porous materials, composed of metal ions or metal clusters with multitopic organic ligands, usually thermally robust and have nanoporous spaces that could be accessed by guest molecules.[6-8] Although many studies have demonstrated that the catalytic activity can be enhanced by decreasing the MNP sizes owing to their high surface area and surface roughness, very few studies have shown changes in product selectivity.[1a] Reactant size selectivity during catalytic transformation is now common phenomenon in porous material-based catalysts, modulated by the pore sizes of used porous support.[9] Recently MNP size- and location-controlled activity has been reported with MOF as support,[5a] whereas controlling of reaction pathway and product selectivity by the surfactant-free MNP size and location have not yet been attempted with any porous host materials.

In the past decades, production of fuels from renewable biomass has drawn considerable attention.[10] The continued depletion of fossil fuels has marked serious concerns for searching renewable and sustainable fuel sources. Lignin, which constitutes ~30 wt % of woody biomass, is the second most abundant bio-source on earth after cellulose.[11] Compared to cellulose-derived pyrolysis oil, it is more challenging to deoxygenate lignin-derived pyrolysihs oil because of its higly complicated structure, which consists of oxygen-rich subunits derived from phenol, p-coumaryl, coniferyl, and sinapyl alcohols typically connected with ether linkages. Hydrodeoxygenation is one of the best ways to improve the quality of biofuels; however, a suitable catalyst with high activity is always demanded.[12] In this regard, ultrafine MNPs immobilized within pores could provide highly active sites for decreasing the oxygen contents from bio-oils by hydrodeoxygenation reaction.

Herein, we chose vanillin (4-hydroxy-3-methoxybenzaldehyde), a large component of pyrolysis oil derived from the lignin fraction, as a reactant to study the catalytic hydrodeoxygenation reaction with MOF-immobilized Pd NPs. Although reactant's size and shape selectivity with porous material-based catalysts have been successfully reported thus far, to the best of our knowledge, for any catalytic organic reactions, this is the first example that location and size of MNPs immobilized into nanopores can control the reaction pathway and product selectivity. Scheme 1 shows the immobilization of Pd nanoparticles into/onto MIL-101 and their use for one- and two-step catalytic hydrodeoxygenation reactions of vanillin.

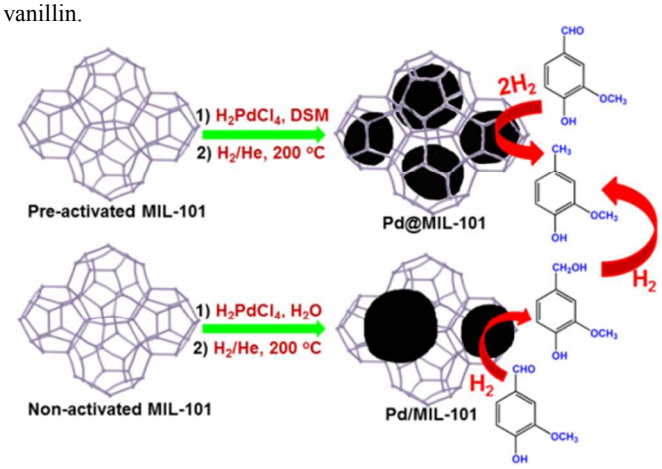


**Scheme 1** Schematic representation of the immobilization of Pd nanoparticles into/onto MIL-101, and their use for catalytic hydrodeoxygenation reactions of vanillin.

MIL-101, a chromium-based MOF with molecular formula $Cr_3F(H_2O)_2O[(O_2C)C_6H_4(CO_2)]_3.nH_2O$ ($n$ = ~25), was chosen for immobilizing MNPs because of its high stability in water, large surface area, and two giant zeotypic cavities with free diameters of 2.9 and 3.4 nm accessible through two pore windows of 1.2 and 1.6

nm.[13] Double solvents method (DSM) was used to immobilize ultrafine Pd NPs within MIL-101 cavities,[5b] while simple deposition of Pd precursor on non-activated MIL-101 led to larger and outer-surface deposited Pd NPs.[14] Briefly, for loading Pd NPs inside the cavities of MIL-101, 100 mg of green MIL-101 powder activated by heating at 150 °C for overnight under vacuum was suspended in hexane (20 mL), to which an aqueous $H_2PdCl_4$ solution (0.15 mL) with required concentrations was added dropwise under continuous vigorous stirring. After careful filtration, the green powder was dried in air at room temperature followed by further drying at 150 °C for overnight and subsequent reduction in a stream of $H_2$/He (50:50 mL $min^{-1}$) at 200 °C for 5 h to yield the sample designated as Pd@MIL-101. For immobilizing Pd NPs to the outer surfaces of MIL-101, 100 mg of MIL-101 without pre-activation was mixed with aqueous $H_2PdCl_4$ solution (0.5 mL) by stirring. After drying at room temperature, the green powder was further dried at 150 °C for overnight and subsequently reduced in a stream of $H_2$/He (50:50 mL $min^{-1}$) at 200 °C for 5 h to yield the sample designated as Pd/MIL-101.[14]

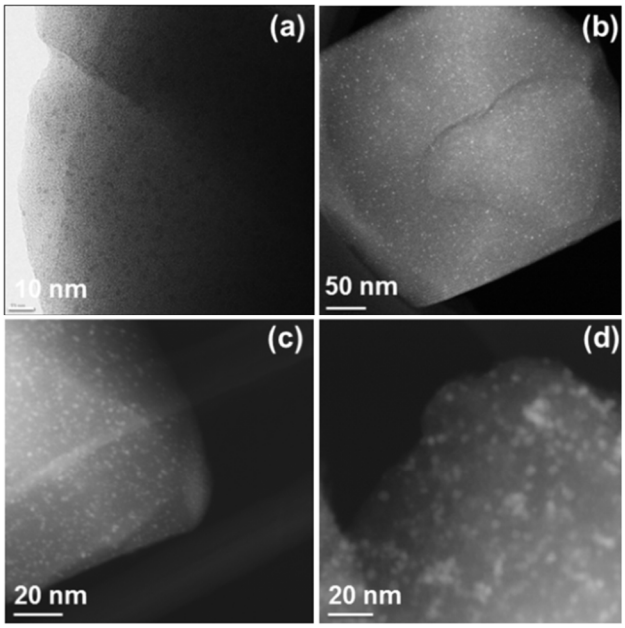


**Fig. 1** (a) TEM and (b, c) HAADF-STEM images of Pd@MIL-101; (d) HAADF-STEM image of Pd/MIL-101.

There was no loss of crystallinity in the powder X-ray diffraction (PXRD) patterns after reduction, suggesting that the integrity of the MIL-101 framework was maintained after MNP deposition in Pd@MIL-101 (Fig. S1). The decreases in the amount of $N_2$ adsorption and the pore volume indicated that the cavities of MIL-101 were occupied by dispersed Pd NPs and/or blocked by the Pd NPs located at the MIL-101 surface (Fig. S2). The X-ray photoelectron spectrum (XPS) of Pd@MIL-101 at Pd 3d levels exhibited metallic Pd peaks (Fig. S3). The high-angle annular dark-field scanning transmission electron microscopy (HAADF-STEM) and transmission electron microscopy (TEM) images (Figs. 1a-1c), energy-dispersive X-ray spectroscopy (EDX) analyses (Fig. S4) and electron tomographic reconstruction (a movie provided as ESI) of Pd@MIL-101 exhibited the three-dimensional uniformity of the Pd NPs in the cavities of MIL-101 crystalline framework. The TEM images of Pd@MIL-101 showed that the sizes of the Pd NPs were in the range of 1.0-2.2 nm with an average size of 1.8 ± 0.2 nm, which are small enough to be accommodated in the two mesoporous cavities of MIL-101; no large Pd particle aggregations have been observed in the TEM and STEM images. High resolution STEM (HRSTEM) analysis showed that the Pd NPs are crystalline with an average spacing of 2.4 Å corresponding to Pd (1 1 1) (Fig. S5). On the other hand, STEM images of Pd/MIL-101 showed broad distribution of larger Pd NPs throughout the outer surfaces of MIL-101 with an average size of 5.0 ± 0.5 nm, larger than the cavity sizes of MIL-101 (Fig. 1d), while PXRD and BET measurements of Pd/MIL-101 suggested the retention of MIL-101 framework (Figs. S1, S2).

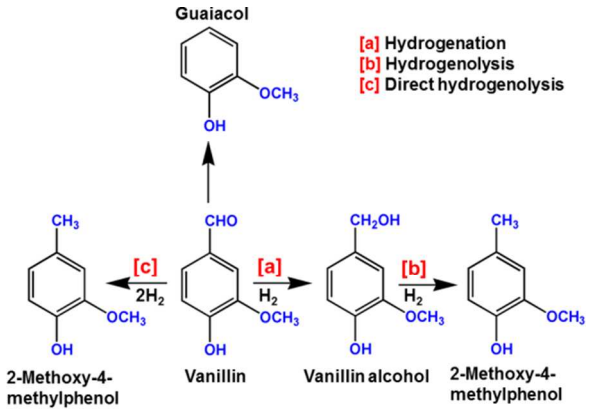


**Scheme 2** Possible reaction pathways for vanillin hydrodeoxygenation.

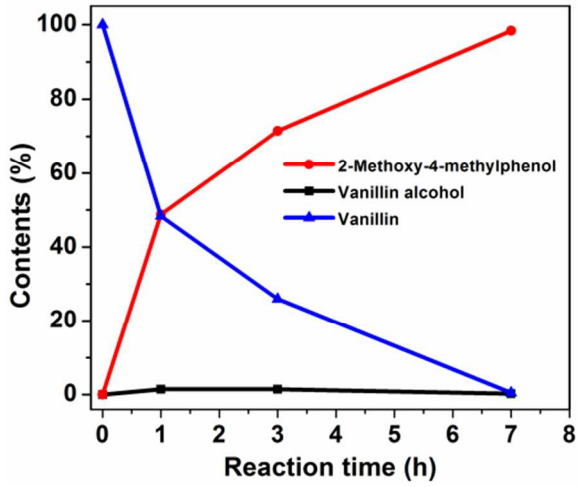


**Fig. 2** Evolution of reactant and products contents with reaction time in the reaction of vanillin over 2 wt% Pd immobilized inside the cavity of MIL-101 (Pd@MIL-101) at 75 °C and 2 bar $H_2$.

To examine the catalytic activity of Pd@MIL-101, biofuel upgrade was investigated in aqueous medium. Water is a desirable green solvent for chemical transformations for reasons of cost, safety, and environmental impacts. Vanillin, a large component of pyrolysis oil derived from the lignin fraction, was chosen as a reactant to study the catalytic hydrodeoxygenation reaction.[14] Transformation of carbonyl group into a methyl group can proceed in three pathways: (1) hydrogenation/dehydration, (2) hydrogenation/hydrogenolysis, and (3) direct hydrogenolysis.[15] Since after hydrogenation vanillin alcohol has no hydrogen atom at the adjacent position to the hydroxyl group, dehydration is not possible in this reaction. Therefore, the transformation of vanillin to 2-methoxy-4-methylphenol must proceed via pathway (2) and/or pathway (3) (Scheme 2). Fig. 2 shows the evolution of the reactant and products contents with the reaction time. The catalytic reaction was carried out in a stainless steel reactor inbuilt with a pressure gauge setup.

The contents of products and reactant were determined by GC-FID based on authentic samples. Briefly, vanillin (100 mg), Pd@MIL-101 catalyst (100 mg, 2 wt% Pd) and water (5 mL) were added into the reactor. The reactor was evacuated with vacuum pump for 15 min at room temperature to remove any $O_2$ or air and then pressurized with $H_2$ at a desired pressure. The temperature of the reactor was maintained with heating bath. After reaction, the reactor was removed from the heating bath and cooled down to room temperature. Ethyl acetate was used to extract the organic compounds from aqueous solution and then condensed and solved in ethanol before supplied for GC-FID analysis.[14] The reaction was accompanied by almost proportional increase and decrease in 2-methoxy-4-methylphenol and vanillin, respectively, with only a very small amount of vanillin alcohol (~ 2%) observed in initial 3 h, suggesting that mainly the direct hydrogenolysis of vanillin occurred (Fig. 2). The transformation into 2-methoxy-4-methylphenol was completed in 7 h (Fig. S6). These observations were consistent with both ethyl acetate and aqueous phases GC analysis (Figs. S7, S8). This finding, associated with ultrafine Pd NPs embedded within the MOF pores, is different from the very recently reported observations associated with larger MNPs dispersed on the surfaces of carbon supports.[16] In these recent studies, the conversion of vanillin to 2-methoxy-4-methylphenol proceeded with hydrogenation to vanillin alcohol followed by hydrogenolysis. For example, in a biphasic system (water and decalin) the Pd@SWNT-$SiO_2$ catalyst afforded a 82% conversion of vanillin in 1 h at 100 $^oC$ with 17 and 83 % selectivities for 2-methoxy-4-methylphenol and vanillin alcohol, respectively.[16b] With similar kinetics, Wang and co-workers demonstrated 90% vanillin conversion at 90 $^oC$ and 1 bar $H_2$ in water with 22 and 78 % selectivities for 2-methoxy-4-methylphenol and vanillin alcohol, respectively, over nitrogen-doped carbon-immobilized Pd catalyst (Pd@$CN_{0.132}$).[16a] In comparison to these reports, Pd@MIL-101 has higher catalytic activity with 49% conversion in initial 1 h with ~100 % selectivity for 2-methoxy-4-methylphenol under very mild conditions (75 $^oC$ and 2 bar $H_2$).

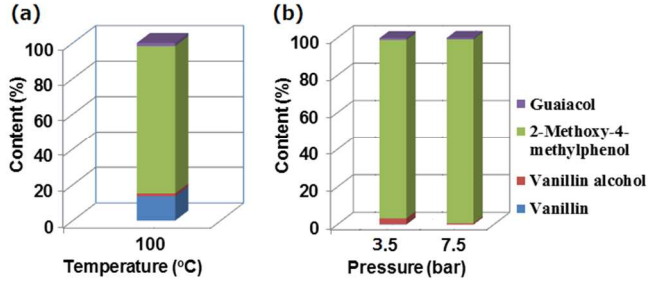


**Fig. 3** Reactant and products distributions with Pd@MIL-101 for vanillin hydrogenolysis for 2 h reaction time at (a) 100 $^oC$ (2 bar $H_2$ pressure) and (b) different $H_2$ pressures (75 $^oC$).

We subsequently conducted the reaction at higher temperature and pressure, and observed enhanced reaction rates in both cases. As shown in Fig. 3, raising the temperature or pressure led to higher rate of vanillin conversion to 2-methoxy-4-methylphenol without observing any significant formation of vanillin alcohol. However, at higher temperature some decarbonylation of the aldehyde group was observed, leading to a deeper hydrogenolysis product o-methoxyphenol (guaiacol).

On the other hand, Pd/MIL-101 which has larger Pd size and is located on the outer surfaces of MIL-101, showed the formation of significant amounts of vanillin alcohol under similar conditions, following the reaction path of previously reported Pd/Carbon based catalysts. The reaction was accompanied by formation of vanillin alcohol in initial hours (26% conversion in 3 h at 75 $^oC$ and 2 bar $H_2$) via hydrogenation, which was subsequently converted to 2-methoxy-4-methylphenol via hydrogenolysis (Fig. 4, S9). Even at 3 h of reaction, 25% of vanillin itself was observed, suggesting that hydrogenolysis of vanillin alcohol together with vanillin direct hydrogenolysis occurred, ie, the process is not selective for any of available two paths.

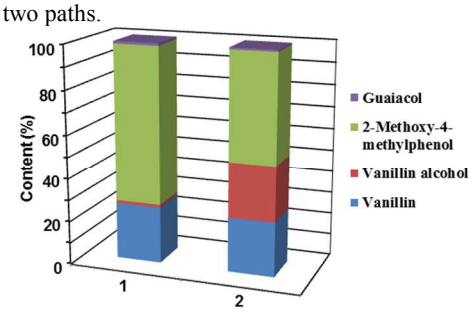


**Fig. 4** Reactant and products distributions for vanillin hydrodeoxygenation under identical conditions (2 bar $H_2$, 75 $^oC$, 3 h) with (1) Pd@MIL-101 and (2) Pd/MIL-101.

The higher activity of Pd@MIL-101 might be owing to the smaller size of Pd NPs confined within the cavities of the MIL-101. The striking selectivity of Pd@MIL-101 for 2-methoxy-4-methylphenol via direct hydrogenolysis could be associated with the steric hindrance and strong interactions of the reactant and intermediate (vanillin alcohol) caused by the encapsulation of ultrafine Pd within the MIL-101 cavities, which resulted in the blocking of the reaction pathway to vanillin alcohol by steric constraints. Without any nano-confinement effect Pd is better accessible in case of Pd/MIL-101, which leads to weak interactions with the reactant and thus results in the observed higher quantity of vanillin alcohol. It is proposed that the adsorbate-surface interactions become stronger over smaller nanoparticles and, other than catalytic activity, dramatic changes in product selectivity occur with MNPs in the size region of 1-10 nm.[1] Therefore, other than nanoconfinement and strong reactant-catalyst interaction effects, the Pd particle size could also be a determining factor for such higher selectivity, as Pd in Pd@MIL-101 has much smaller sizes (~1.8 nm) than those in Pd/MIL-101 and the previously reported Pd/carbon based catalysts (~5 nm). Furthermore, Pd@MIL-101 can be easily separated from the reaction solution by simple filtration. The catalyst showed high stability and could be reused for several cycles with complete conversion of vanillin. After catalytic reactions, the crystallinities of MIL-101 frameworks as well as metallic Pd state remain unchanged, as confirmed by the PXRD and XPS patterns, respectively (Figs. S10, S11). TEM measurements of Pd@MIL-101 after catalysis showed no significant changes in the size and morphologies of Pd NPs with retention of the MIL-101 framework (Fig. S12). The ultrafine sub-2 nm sizes of the Pd stably immobilized within MIL-101 zeotypic cavities with exposed (111) planes largely contributed to the high catalytic activities.

In conclusion, ultrafine Pd NPs have been immobilized within the cavities of a mesoporous MOF, MIL-101, which showed high activity and selectivity for the hydrodeoxygenation of vanillin, a common component in lignin-derived bio-oil, under mild reaction conditions with water as a green solvent. The high catalytic performance has been attributed to the nano-confinement effect and strong interactions between reactants and confined Pd NPs. This is a good example showing the significance of size/location of MNPs immobilized to nanoporous materials. The present results bring light to new opportunities in the development of high performance heterogeneous catalysts for more selective organic transformations. These catalysts hold promising potential for biofuel upgrade processes, and further work will be directed toward the applications to natural lignin and other model compounds.

The authors are thankful to Dr. Takeyuki Uchida for TEM measurements, and AIST and JSPS for financial support. A.A. thanks JSPS for a postdoctoral fellowship.

## Notes and references

[a]National Institute of Advanced Industrial Science and Technology (AIST), Ikeda, Osaka 563-8577, Japan. E-mail: q.xu@aist.go.jp
[b]Toyama National College of Technology, 13, Hongo-machi, Toyama, 939-8630, Japan

† Electronic Supplementary Information (ESI) available: Detailed experimental conditions and procedures, catalytic and characterization data, more TEM images and a tomographic movie for Pd@MIL-101. See DOI: 10.1039/c000000x/

1 (a) K. An and G. A. Somorjai, *ChemCatChem*, 2012, **4**, 1512; (b) G. A. Somorjai and J. Y. Park, *Angew. Chem., Int. Ed.*, 2008, **47**, 9212.
2 (a) C. Chen, Y. Kang, Z. Huo, Z. Zhu, W. Huang, H. L. Xin, J. D. Snyder, D. Li, J. A. Herron, M. Mavrikakis, M. Chi, K. L. More, Y. Li, N. M. Markovic, G. A. Somorjai, P. Yang and V. R. Stamenkovic, *Science*, 2014, **343**, 1339; (b) R. V. Jagadeesh, A. E. Surkus, H. Junge, M. M. Pohl, J. Radnik, J. Rabeah, H. Huan, V. Schunemann, A. Bruckner and M. Beller, *Science*, 2013, **342**, 1073; (c) X. W. Xie, Y. Li, Z. Q. Liu, M. Haruta and W. J. Shen, *Nature*, 2009, **458**, 746.
3 (a) A. Zhao, J. Masa, W. Xia, A. Maljusch, M.-G. Willinger, G. Clavel, K. Xie, R. Schlögl, W. Schuhmann and M. Muhler, *J. Am. Chem. Soc.*, 2014, **136**, 7551; (b) R. J. White, R. Luque, V. L. Budarin, J. H. Clark and D. J. Macquarrie, *Chem. Soc. Rev.*, 2009, **38**, 481.
4 (a) A. Aijaz and Q. Xu, *J. Phys. Chem. Lett.*, 2014, **5**, 1400; (b) H. R. Moon, D.-W. Limb and M. P. Suh, *Chem. Soc. Rev.*, **2013**, *42*, 1807; (c) A. Dhakshinamoorthy and H. Garcia, *Chem. Soc. Rev.*, 2012, **41**, 5262; (d) M. Meilikhov, K. Yusenko, D. Esken, S. Turner, G. Van Tendeloo and R. A. Fischer, *Eur. J. Inorg. Chem.*, 2010, 3701.
5 (a) Y. Huang, Y. Zhang, X. Chen, D. Wu, Z. Yi and R. Cao, *Chem. Commun.*, 2014, **50**, 10115; (b) Q.-L. Zhu, J. Li and Q. Xu, *J. Am. Chem. Soc.*, 2013, **135**, 10210; (c) A. Aijaz, A. Karkamkar, Y. Joon Choi, N. Tsumori, E. Rönnebro, T. Autrey, H. Shioyama and Q. Xu, *J. Am. Chem. Soc.*, 2012, **134**, 13926; (d) J. Hermannsdörfer, M. Friedrich, N. Miyajima, R. Q. Albuquerque, S. Kümmel and R. Kempe, *Angew. Chem., Int. Ed.*, 2012, **51**, 11473; (e) Y. Wei, S. Han, D. A. Walker, P. E. Fuller and B. A. Grzybowski, *Angew. Chem., Int. Ed.*, 2012, **51**, 7435; (f) Y. Huang, Z. Lin and R. Cao, *Chem.-Eur. J.*, 2011, **17**, 11706; (g) R. Ameloot, M. B. J. Roeffaers, G. De Cremer, F. Vermoortele, J. Hofkens, B. F. Sels and D. E. De Vos, *Adv. Mater.*, 2011, **23**, 1788; (h) D. Esken, S. Turner, O. I. Lebedev, G. Van Tendeloo and R. A. Fischer, *Chem. Mater.*, 2010, **22**, 6393; (i) M. Sabo, A. Henschel, H. Froede, E. Klemm and S. Kaskel, *J. Mater. Chem.*, 2007, **17**, 3827; (j) S. Hermes, M.-K. Schrçter, R. Schmid, L. Khodeir, M. Muhler, A. Tissler, R.W. Fischer and R. A. Fischer, *Angew. Chem. Int. Ed.*, 2005, **44**, 6237.
6 (a) H. C. Zhou, J. R. Long and O. M. Yaghi, *Chem. Rev.*, 2012, **112**, 673; (b) N. Stock and S. Biswas, *Chem. Rev.*, **2012**, *112*, 933; (c) B. Chen, S. Xiang and G. Qian, *Acc. Chem. Res.*, 2010, **43**, 1115; (d) O. K. Farha and J. T. Hupp, *Acc. Chem. Res.*, 2010, **43**, 1166; (e) G. Férey, *Chem. Soc. Rev.*, 2008, **37**, 191; (f) S. Kitagawa, R. Kitaura and S. Noro, *Angew. Chem., Int. Ed.*, 2004, **43**, 2334.
7 (a) H. Furukawa, K. E. Cordova, M. O'Keeffe and O. M. Yaghi, *Science*, 2013, **341**, 1230444; (b) J.-R. Li, J. Sculley and H.-C. Zhou, *Chem. Rev.*, 2012, **112**, 869; (c) Scott T. Meek, J. A. Greathouse and M. D. Allendorf, *Adv. Mater.*, 2011, **23**, 249; (d) A. Corma, H. Garcia and F. X. L. I. Xamena, *Chem. Rev.*, 2010, **110**, 4606; (e) L. Ma, C. Abney and W. Lin, *Chem. Soc. Rev.*, 2009, **38**, 1248; (f) G. K. H. Shimizu, R. Vaidhyanathan and J. M. Taylor, *Chem. Soc. Rev.*, 2009, **38**, 1430.
8 (a) G. Li, H. Kobayashi, J. M. Taylor, R. Ikeda, Y. Kubota, K. Kato, M. Takata, T. Yamamoto, S. Toh, S. Matsumura and H. Kitagawa, *Nature Mater.*, 2014, **13**, 802; (b) A. Santra, I. Senkovska, S. Kaskel and P. K. Bharadwaj, *Inorg. Chem.*, 2013, **52**, 7358; (c) A. Mallick, B. Garai, D. D. Díaz and R. Banerjee, *Angew. Chem. Int. Ed.*, 2013, **52**, 13755; (d) S. Sen, N. N. Nair, T. Yamada, H. Kitagawa and P. K. Bharadwaj, *J. Am. Chem. Soc.*, 2012, **134**, 19432; (e) G.-Q. Kong, S. Ou, C. Zou and C.-D. Wu, *J. Am. Chem. Soc.*, 2012, **134**, 19851; (f) C.-H. Kuo, Y. Tang, L.-Y. Chou, B. T. Sneed, C. N. Brodsky, Z. Zhao and C.-K. Tsung, *J. Am. Chem. Soc.*, 2012, **134**, 14345; (g) K. Gedrich, I. Senkovska, N. Klein, U. Stoeck, A. Henschel, M. R. Lohe, I. A. Baburin, U. Mueller and S. Kaskel, *Angew. Chem., Int. Ed.*, 2010, **49**, 8489.
9 (a) M. Zhao, S. Ou and C.-D. Wu, *Acc. Chem. Res.*, 2014, **47**, 1199; (b) M. Yoon, R. Srirambalaji and K. Kim, *Chem. Rev.*, 2012, **112**, 1196.
10 (a) P. Gallezot, *Chem. Soc. Rev.*, 2012, **41**, 1538; (b) D. M. Alonso, J. Q. Bond and J. A. Dumesic, *Green Chem.*, 2010, **12**, 1493.
11 A. J. Ragauskas, G. T. Beckham, M. J. Biddy, R. Chandra, F. Chen, M. F. Davis, B. H. Davison, R. A. Dixon, P. Gilna, M. Keller, P. Langan, A. K. Naskar, J. N. Saddler, T. J. Tschaplinski, G. A. Tuskan and C. E. Wyman, *Science*, 2014, **344**, 709.
12 M. Saidi, F. Samimi, D. Karimipourfard, T. Nimmanwudipong, B. C. Gates and M. R. Rahimpour, *Energy Environ. Sci.*, 2014, **7**, 103.
13 G. Férey, C. Mellot-Draznieks, C. Serre, F. Millange, J. Dutour, S. Surblé and I. Margiolaki, *Science*, 2005, **309**, 2040.
14 See the electronic supplementary information (ESI).
15 D. Prochazkova, P. Zamostny, M. Bejblova, L. Cerveny and J. Cejka, *Appl. Catal. A*, 2007, **332**, 56.
16 (a) X. Xu, Y. Li, Y. Gong, P. Zhang, H. Li, Y. Wang, *J. Am. Chem. Soc.*, 2012, **134**, 16987; (b) S. Crossley, J. Faria, M. Shen and D. E. Resasco, *Science*, 2010, **327**, 68.



 